



---

Time- and Space-Resolved Spectroscopic Investigation on Pi-Conjugated Nanostructures - 2

Dongho Kim  
YONSEI UNIVERSITY UNIVERSITY-INDUSTRY FOUNDATION

---

02/02/2016  
Final Report

DISTRIBUTION A: Distribution approved for public release.

Air Force Research Laboratory  
AF Office Of Scientific Research (AFOSR)/ IOA  
Arlington, Virginia 22203  
Air Force Materiel Command

**REPORT DOCUMENTATION PAGE**

Form Approved  
OMB No. 0704-0188

The public reporting burden for this collection of information is estimated to average 1 hour per response, including the time for reviewing instructions, searching existing data sources, gathering and maintaining the data needed, and completing and reviewing the collection of information. Send comments regarding this burden estimate or any other aspect of this collection of information, including suggestions for reducing the burden, to Department of Defense, Washington Headquarters Services, Directorate for Information Operations and Reports (0704-0188), 1215 Jefferson Davis Highway, Suite 1204, Arlington, VA 22202-4302. Respondents should be aware that notwithstanding any other provision of law, no person shall be subject to any penalty for failing to comply with a collection of information if it does not display a currently valid OMB control number.

**PLEASE DO NOT RETURN YOUR FORM TO THE ABOVE ADDRESS.**

<b>1. REPORT DATE (DD-MM-YYYY)</b> 23-06-2016		<b>2. REPORT TYPE</b> Final		<b>3. DATES COVERED (From - To)</b> 25-09-2014 to 24-09-2015	
<b>4. TITLE AND SUBTITLE</b>  Time- and Space-Resolved Spectroscopic Investigation on Pi-Conjugated Nanostructures - 2				<b>5a. CONTRACT NUMBER</b> FA2386-14-1-4102	
				<b>5b. GRANT NUMBER</b> Grant AOARD-144102	
				<b>5c. PROGRAM ELEMENT NUMBER</b>	
<b>6. AUTHOR(S)</b>  Prof Dongho Kim				<b>5d. PROJECT NUMBER</b>	
				<b>5e. TASK NUMBER</b>	
				<b>5f. WORK UNIT NUMBER</b>	
<b>7. PERFORMING ORGANIZATION NAME(S) AND ADDRESS(ES)</b> Yonsei University Shinchon-Dong 134, Seodaemoon-Ku Seoul 120-749 Korea (South)				<b>8. PERFORMING ORGANIZATION REPORT NUMBER</b>  N/A	
<b>9. SPONSORING/MONITORING AGENCY NAME(S) AND ADDRESS(ES)</b>  AOARD UNIT 45002 APO AP 96338-5002				<b>10. SPONSOR/MONITOR'S ACRONYM(S)</b>  AOARD	
				<b>11. SPONSOR/MONITOR'S REPORT NUMBER(S)</b> AOARD-144102	
<b>12. DISTRIBUTION/AVAILABILITY STATEMENT</b>  Approved for public release.					
<b>13. SUPPLEMENTARY NOTES</b>					
<b>14. ABSTRACT</b> Highly conjugated pi-molecular systems show attractive semiconducting and optical properties, which makes them highly attractive materials for applications in organic electronic devices and molecular electronics as their optical phenomena may be manipulated in ways not possible with bulk materials. This research investigates photophysical properties of fused linear and macrocyclic porphyrin arrays by integrated time- and space-resolved spectroscopic methodologies to understand the effect of pi-conjugation and molecular structure in excited-state dynamic systems. This is the first study to demonstrate that the electronic deactivation overtakes vibrational relaxation processes in the energy relaxation processes from initially excited vibronic state manifolds in highly conjugated molecular systems. The report also includes an examination of structural properties and fluorescent trapping sites at the single-molecule level. Defocused wide-field fluorescence (DWFI) microscopy suggests that molecular heterogeneities and flexibilities clearly depend on ring size and that site selection for fluorescent trapping is related to the nature of the surrounding chromophore environment. The direct observation of prevailing molecular conformations and the location of fluorescent trapping sites in multichromophoric macrocycles using single-molecule spectroscopic methods provides not only a new level of understanding, but will also stimulate other experimental and computational studies on related multichromophoric systems.					
<b>15. SUBJECT TERMS</b> Materials Characterization, Materials Chemistry, Nonlinear Optical Materials, Spectroscopy					
<b>16. SECURITY CLASSIFICATION OF:</b>			<b>17. LIMITATION OF ABSTRACT</b>	<b>18. NUMBER OF PAGES</b>	<b>19a. NAME OF RESPONSIBLE PERSON</b>
<b>a. REPORT</b>	<b>b. ABSTRACT</b>	<b>c. THIS PAGE</b>			Kenneth Caster, Ph.D.
U	U	U	SAR	14	<b>19b. TELEPHONE NUMBER (Include area code)</b> +81-3-5410-4409

**Final Report for AOARD Grant**

**Time- and Space-Resolved Spectroscopic  
Investigation on  
 $\pi$ -Conjugated Nanostructures**

*12<sup>th</sup> January 2016*

- **Name of Principal Investigator:** Dongho Kim
- **E-mail Address:** dongho@yonsei.ac.kr
- **Institution:** Department of Chemistry, Yonsei University
- **Mailing Address:** Shinchon-dong 134, Seodaemun-gu, Seoul 120-749, Korea
- **Tel:** +82-2-2123-2652
- **Fax:** +82-2-2123-2434
- **Home Page:** <http://www.fpieslab.com/>
- **Period of Performance:** September/25/2014 – September/24/2015

## Table of Contents

<b>1. Cover Page.....</b>	<b>1</b>
<b>2. Table of Contents.....</b>	<b>2</b>
<b>3. Abstract.....</b>	<b>3</b>
<b>4. Introduction.....</b>	<b>4</b>
<b>5. Experiment.....</b>	<b>6</b>
<b>6. Results and Discussion.....</b>	<b>8</b>
<b>7. Publication List.....</b>	<b>12</b>

## Abstract

$\pi$ -Conjugated molecular systems show attractive semiconducting and optical properties, which makes them highly attractive materials with a great potential for applications in organic electronic devices and molecular electronics. Therefore, the study of functional  $\pi$ -electronic molecular systems touches almost every aspect of synthetic, theoretical, and physical chemistry. In this regard, we have investigated the photophysical properties of various  $\pi$ -electronic molecular systems, such as fused linear and macrocyclic porphyrin arrays by integrated time- and space-resolved spectroscopic methodologies.

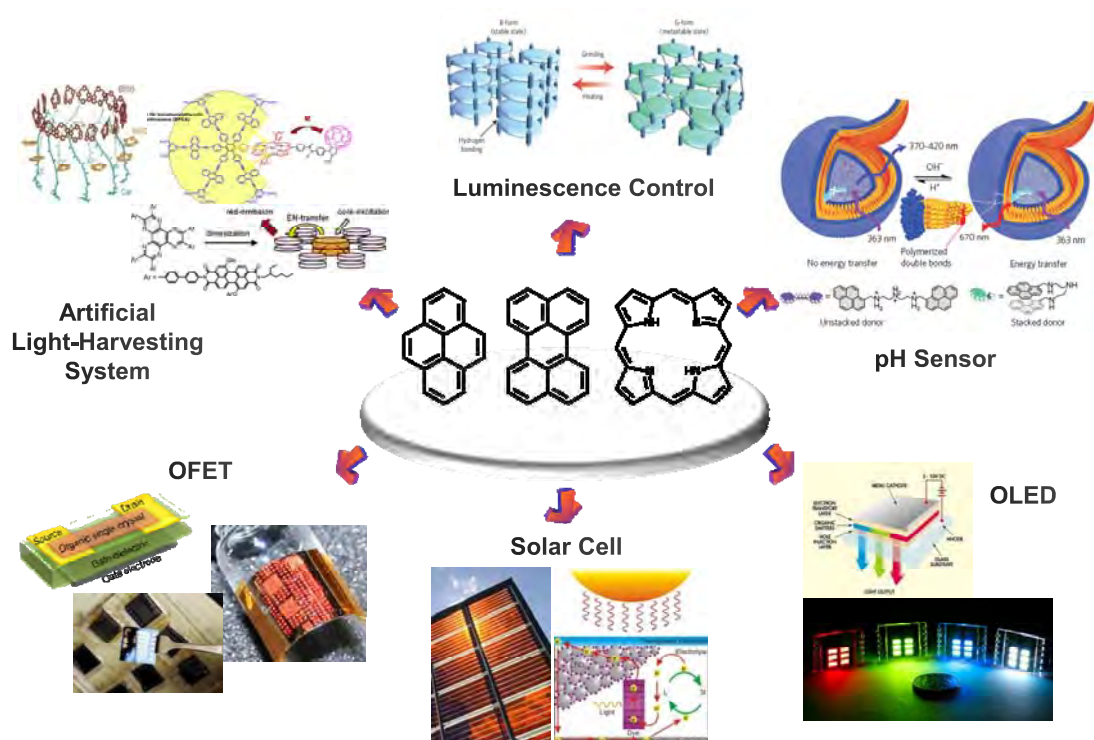


**Figure 1.** Various applications of  $\pi$ -conjugated molecular systems

## Introduction

$\pi$ -Conjugated nanostructures designed for the manipulation of optical phenomena are of particular interest for a variety of applications that are not possible with bulk materials. For example, (1) light-harvesting nanostructures can be used as energy sources to power molecular devices, (2) molecular photonic wires and gates can be employed to transmit and manipulate signals in nanoscale information processing systems, and (3) structured composites of absorbers and emitters can serve as nanoscale optical sources or imaging elements. All of these structures represent a broad class of photonic devices whose performance can be controlled at the nanometer level. In this context, a detailed understanding of photophysical properties is crucial for the fabrication of novel  $\pi$ -conjugated systems targeted for specific application.

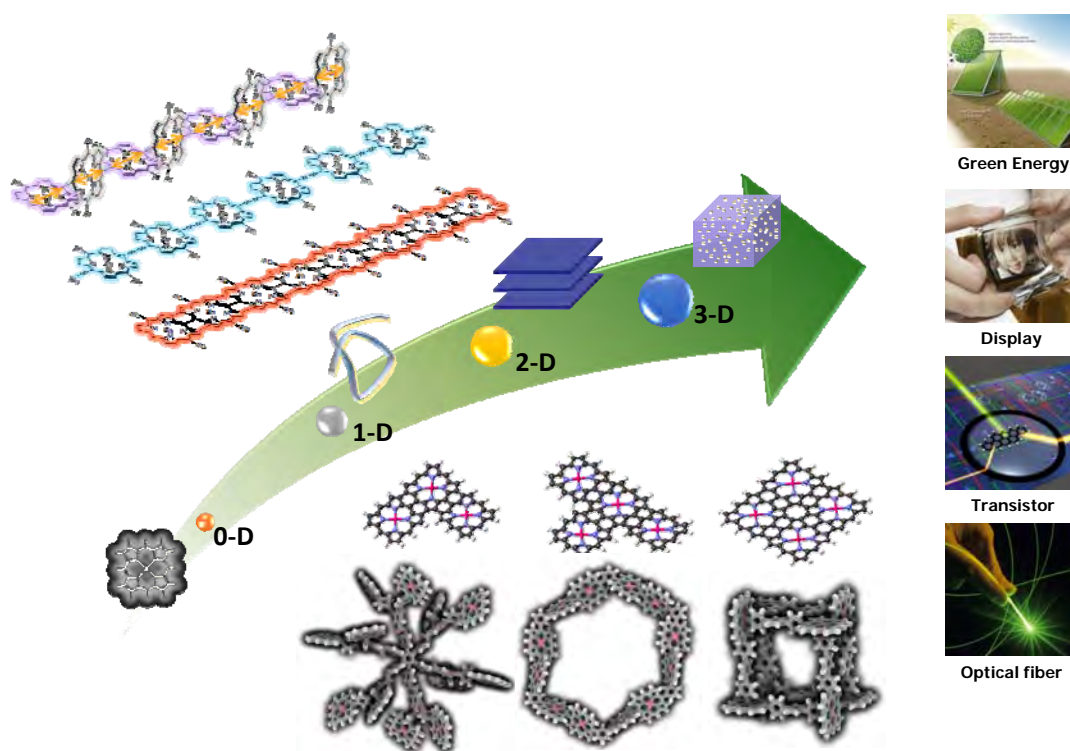


**Figure 2.** Examples of molecular structures for  $\pi$ -conjugated porphyrin oligomers

In the study of functional  $\pi$ -electronic molecular systems, we have focused on  $\pi$ -conjugated porphyrin oligomers, which are one of the most extensively studied molecular motifs in light of their high stabilities, strong electronic absorptions in the visible region, emissive properties of certain porphyrins, efficient energy and electron transfer reactions, nonlinear optical properties, and easily tunable optical properties. In particular, since porphyrin oligomers show various photophysical properties by expansion of  $\pi$ -conjugation and molecular structure, it is vital to understand the effect of  $\pi$ -conjugation and molecular

structure in the excited-state dynamics to explore and improve novel functions of porphyrin oligomers. In this regard, the time- and space-resolved spectroscopic investigations have been conducted to characterize the photophysical properties of fused linear and macrocyclic porphyrin arrays.

The research activity of spectroscopic characterization will empower us to modulate or enhance selectively the functional properties of the  $\pi$ -conjugated nanostructures, which could provide the means for answering a number of addressing certain practical goals, namely how to achieve practical molecular FETs, super-bright LED, and organic laser devices. Given this expectation, we believe our research on  $\pi$ -conjugated nanostructures will translate into new ground-breaking developments that not only allow the structure-property relationships to be probed in greater detail, but also give rise to a number of real-world applications. Consequently, with an active control of  $\pi$ -conjugation and molecular structure, this work has explored the excited-state dynamics of various  $\pi$ -conjugated molecular systems by using various spectroscopic measurements.

# Experiment

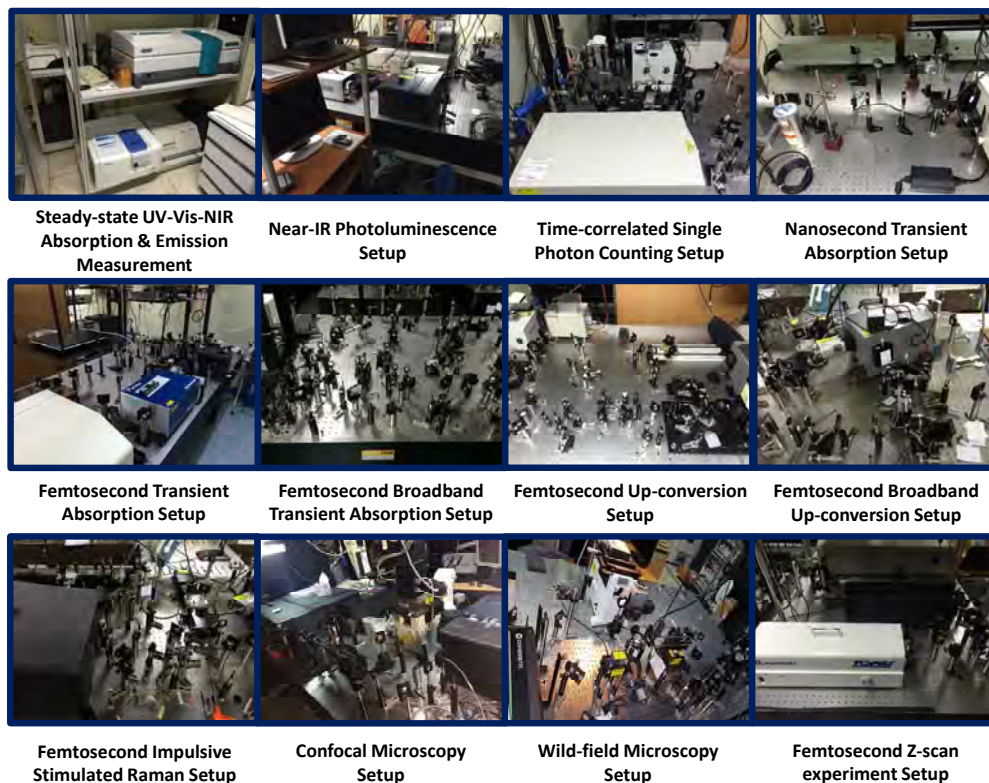


Figure 3. Instruments of Time- and space-resolved spectroscopy.

## I. Experimental method

### 1. Steady-state Spectroscopy

- UV-Vis-NIR Absorption & Emission Steady-state Spectroscopy
- NIR Photoluminescence Spectroscopy

### 2. Time-Resolved Laser Spectroscopy

- Time-Correlated Single Photon Counting (TCSPC) Method
- Nanosecond Transient Absorption Spectroscopy
- Femtosecond Transient Absorption Spectroscopy
- Femtosecond Broadband Transient Absorption Spectroscopy
- Femtosecond Up-conversion Spectroscopy
- Femtosecond Broadband Up-conversion Spectroscopy
- Femtosecond Impulsive Stimulated Raman Spectroscopy



### **3. Space-Resolved Laser Spectroscopy**

- Confocal Microscopy
- Wild-field Microscopy

### **4. Non-Linear Spectroscopy**

- Femtosecond Z-scan Method

## **II. Quantum Mechanical Calculation**

1. Nuclear-Independent Chemical Shift (NICS) Values
2. Anisotropy of the Induced Current Density (AICD) Calculation
3. Molecular Orbitals & Electronic Excited-State Excitation Energies

## Results and Discussion

### 1. Unusual excited-state energy relaxation processes in a highly conjugated molecular system.

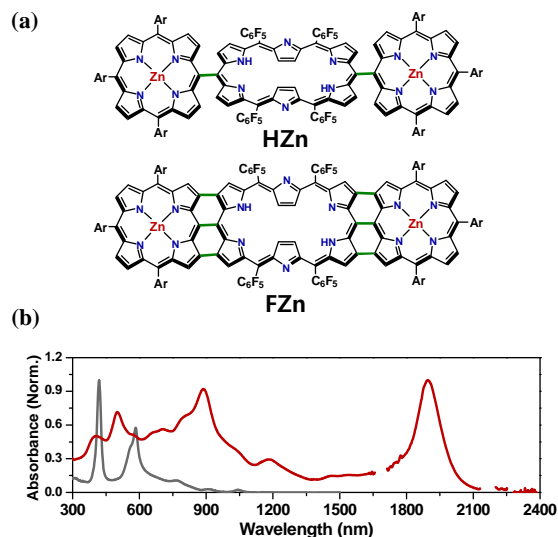


**Figure 4.** (a) Molecular structures of **HZn** and **FZn**; Ar = 3,5-di-tert-butylphenyl (b) Steady-state absorption spectra of **HZn** (gray) and **FZn** (red) in pure toluene and toluene containing 1% pyridine, respectively.

we investigated the excited-state energy relaxation processes of a Zn(II)porphyrin–[26]hexaphyrin–Zn(II)porphyrin triply linked hybrid tape, **FZn**, using a directly *meso–meso* linked hybrid trimer, **HZn**, as a reference compound (Figure 4(a)).

The steady-state absorption spectra of **HZn** and **FZn** taken in pure toluene and toluene containing 1% pyridine at room temperature are shown in Figure 4(b). In contrast to **HZn**, **FZn** has a very small  $S_1$ - $S_0$  energy gap through expansion of  $\pi$ -conjugation, and a absorption band at 1897 nm corresponds to its lowest singlet excited-state as a consequence of enhanced transition dipole moment that lies parallel to the long molecular axis. In TA measurements, we observe a energy transfer process (0.4 ps) from Zn(II)porphyrin moiety to [26]hexaphyrin core in **HZn**. In contrast to **HZn**, biexponential decay with the time constants of 0.25 and 6.5 ps were observed in the decay profile of **FZn**.

To figure out the origin of 0.25 and 5.9 ps decay components in **FZn**, we have measured the excitation wavelength dependent TA spectra by systematically changing the pump wavelength from 420 to 1300 nm (Figure 5). Although we could detect the decay components of 0.25 and 5.9 ps at all excitation wavelengths, we can assume that the fast decay component of 0.25 ps is mainly attributed to the electronic transition and the slow

In general, organic molecular systems with small  $S_1$ - $S_0$  energy gap show shorter excited-state lifetimes than those with larger  $S_1$ - $S_0$  energy gaps due to the acceleration of nonradiative relaxation processes caused by reduced  $S_1$ - $S_0$  energy gaps, which can be interpreted by the energy gap law. However, we conjectured that the rate of  $S_1$ - $S_0$  electronic relaxation process can be faster than the vibrational relaxation processes in well-conjugated molecules with sufficiently small  $S_1$ - $S_0$  energy gaps from our previous studies on fused Zn(II)porphyrin arrays. To confirm our expectation, we have

decay components to the vibrational relaxation processes of **FZn**, respectively from blue shift of the edge of the excited-state absorption spectra in the near-infrared region and decrease of the amplitude of slow decay components (5.9 ps) in the TA decay profiles as the excitation energy decreases. Additionally, we discovered that the slow decay component (5.2 ps) at 77 K is slightly longer than that (4.4 ps) at 297 K, but the fast decay components (0.25 ps) were insensitive to the temperature. Therefore, we can conclude that the fast decay component of 0.25 ps is mainly attributed to the electronic transition and the slow decay components to the vibrational relaxation processes of **FZn**, respectively.

In the absorption spectra of **FZn** and pure toluene, we can find an overlap between the electronic states of **FZn** and the vibrational modes (first overtone of the C—H stretching) of pure toluene. In solvent dependent TA decay profiles, we discovered different slow decay

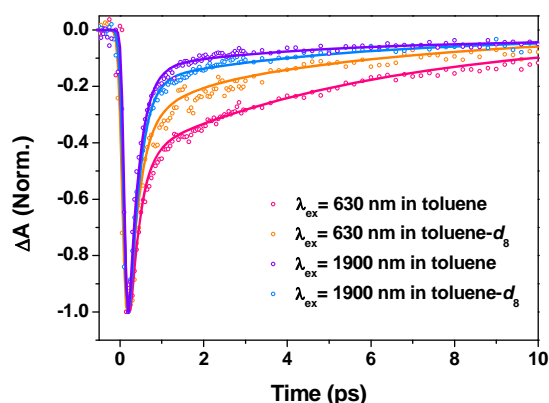


**Figure 6.** Normalized TA decay profiles of **FZn** measured in toluene containing 1% pyridine; green: pump 630 nm; red: pump 1900 nm, and measured in toluene- $d_8$  containing 1% pyridine; blue: pump 630 nm; orange: pump 1900 nm.

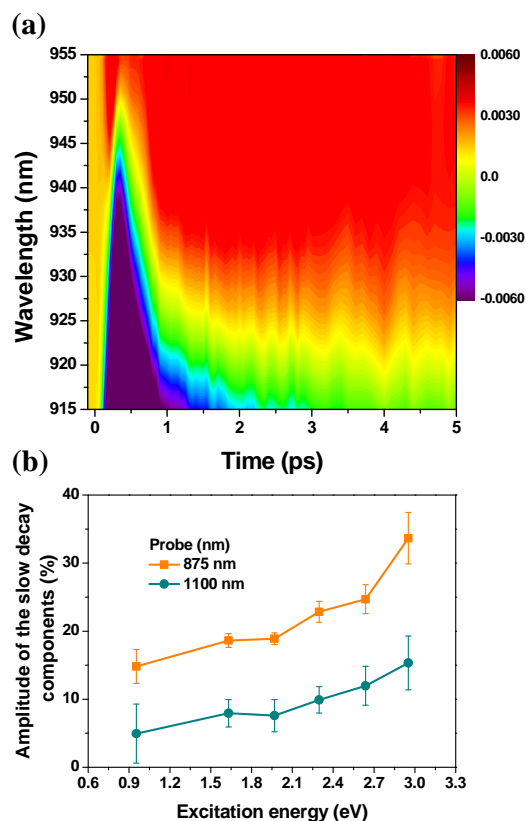


**Figure 5.** (a) Two-dimensional TA contour map of **FZn** with photoexcitation at 630 nm in toluene containing 1% pyridine. (b) Amplitude of the slow decay components in **FZn** probed at 875 and 1100 nm by changing the photoexcitation wavelength from 420 to 1300 nm.

components with time constants of 5.9 and 6.5 ps in toluene and toluene- $d_8$ , respectively (Figure 6). Therefore, we can conclude that the slow decay component in the TA decay profiles of **FZn** corresponding to the vibrational relaxation processes is affected by the intermolecular vibrational energy transfer process in the excited-state of **FZn**.

While the energy relaxation dynamics of large chromophores absorbing in a broad wavelength range have been reported in previous studies, this is the first study, to the best our knowledge, to demonstrate that the

electronic deactivation overtakes the vibrational relaxation processes in the energy relaxation processes from the initially excited vibronic state manifolds in highly conjugated molecular systems just like our **FZn** system.

## 2. Structural properties and fluorescent trapping sites in macrocyclic porphyrin arrays

Molecular electronics technology has been highlighted across science and technology, providing the possibility of constructing photonic devices at the individual molecular level for device miniaturization. The rational design of molecular devices for photonic, electronic, or optoelectronic applications will require an understanding of the molecular structures and ordering among the constituents in multicomponent

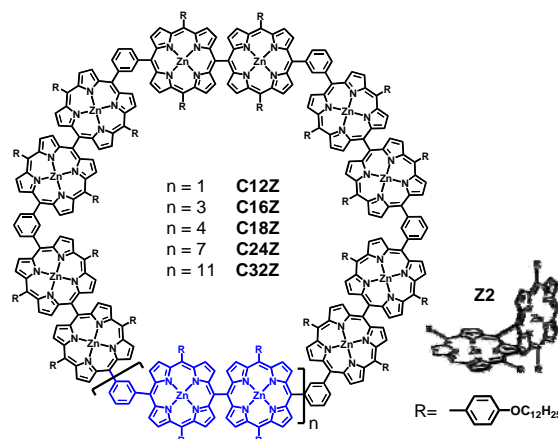


**Figure 7.** Molecular structures of a series of cyclic porphyrin arrays (**CNZs**).

macromolecular architectures: this is because of the close relationship between molecular structures and photophysical properties. Various methods have been utilized to reveal molecular structures at the single-molecule level. One such method is defocused wide-field fluorescence (DWFI) microscopy, which provides information on the three-dimensional orientation of the molecular emission dipole moment. Since DWFI measurements are implemented under slightly defocused condition (about 1  $\mu\text{m}$ ), porphyrin-based molecular systems have scarcely been studied due to their relatively low fluorescence quantum yields. Nevertheless, there have been numerous synthetic trials to produce molecular architectures that mimic the LH1 and LH2 complexes for fabrication of an artificial light-harvesting apparatus. In this regard, we prepared a series of cyclic porphyrin arrays (**CNZs**,  $N = 12, 16, 18, 24$  and  $32$ ; Figure 7), in which *meso-meso* linked Zinc (II) diporphyrin (**Z2**) subunits. According to similar absorption and fluorescence spectral features of a series of **CNZs**, we assumed that the dipole coupling strength among **Z2** units is so weak that **Z2** acts as an individual chromophore.

As shown in Figure 8, the switch from level A to B is accompanied by an intensity drop due to photobleaching of the constituent **Z2** unit. The transition dipole moments for intensity levels A and B were defined to have angles ( $\varphi, \theta$ ) of ( $70^\circ, 85^\circ$ ) and ( $130^\circ, 75^\circ$ ), respectively.

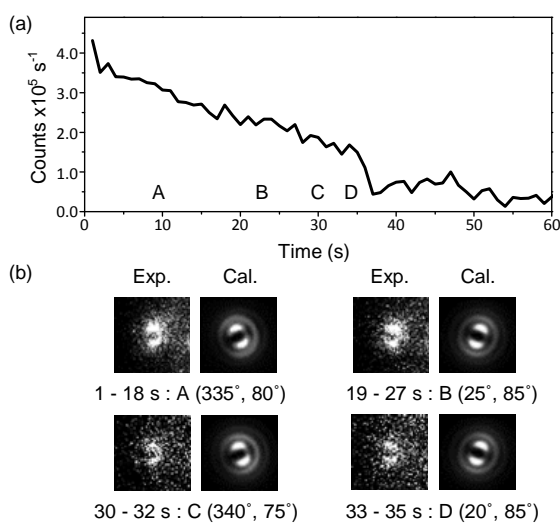


**Figure 8.** Representative example of a single C12Z molecule. (a) Fluorescence intensity trajectory. (b) Experimentally observed defocused images (left) and corresponding calculated images (right) for A – D.

carried out by collecting approximately 80 single-molecule datasets for CNZ to show multiple emission patterns (Figure 9). Our findings suggest that the molecular heterogeneities and flexibilities of CNZs clearly depend on the ring size; as the ring size becomes larger, CNZs become more distorted. Furthermore, we discovered site selection for the fluorescent trapping site in single multichromophoric macrocycles by a comparative analysis between experimental and computational results; the chromophore adjacent to the first fluorescent trapping site has a high probability of being selected as the second fluorescent trapping site due to the similar nature of the surrounding environment. The direct observation of prevailing molecular conformations and the location of fluorescent trapping sites in multichromophoric macrocycles using single-molecule spectroscopic methods provides not only a new level of understanding, but will also stimulate other experimental and computational studies on related multichromophoric systems.

To evaluate the magnitude of the changes in fluorescence polarization direction, we calculated the angle difference between the transition dipole moments from subsequent intensity levels in the FIT using the law of cosines. The calculated angle difference was  $59.8^\circ$ , in excellent agreement with the value of  $60^\circ$  expected from the two-dimensional hexagonal structure.

On the basis of the above observations, a statistical analysis of experimentally observed interchromophoric angles, was

carried out by collecting approximately 80 single-molecule datasets for CNZ to show

multiple emission patterns (Figure 9). Our findings suggest that the molecular heterogeneities and flexibilities of CNZs clearly depend on the ring size; as the ring size becomes larger, CNZs become more distorted.

Furthermore, we discovered site selection for the fluorescent trapping site in single multichromophoric macrocycles by a comparative analysis between experimental and computational results; the chromophore adjacent to the first fluorescent trapping site has a high probability of being selected as the second fluorescent trapping site due to the similar nature of the surrounding environment. The direct observation of prevailing molecular conformations and the location of fluorescent trapping sites in multichromophoric macrocycles using single-molecule spectroscopic methods provides not only a new level of understanding, but will also stimulate other experimental and computational studies on related multichromophoric systems.

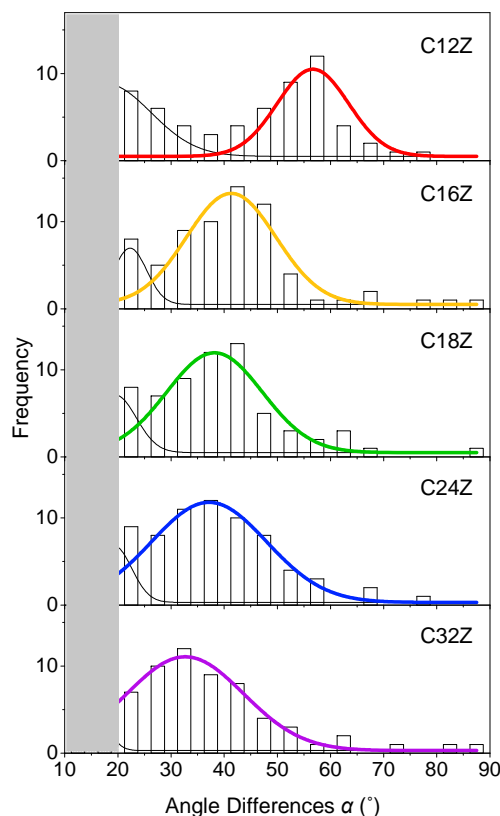


**Figure 9.** Interchromophoric angles Histograms.

## Publication List

**1. Very rapid electronic relaxation process in a highly conjugated Zn(II)porphyrin–[26]hexaphyrin–Zn(II)porphyrin hybrid tape**

Sangsu Lee, Hirotaka Mori, Taegon Lee, Manho Lim, Atsuhiko Osuka and Dongho Kim

*Phys. Chem. Chem. Phys.*, 2016, Accepted Manuscript

**2. Direct observation of structural properties and fluorescent trapping sites in macrocyclic porphyrin arrays at the single-molecule level**

Sujin Ham, Ji-Eun Lee, Suhwan Song, Xiaobin Peng, Takaaki Hori, Naoki Aratani, Atsuhiko Osuka, Eunji Sim and Dongho Kim

*Phys. Chem. Chem. Phys.*, 2016, Accepted Manuscript